Bottom-up Modeling of Residential Heating Systems for Demand Side Management in District Energy System Analysis and Distribution Grid Planning

Michael Kramer, Akhila Jambagi, Vicky Cheng
Munich School of Engineering
Technical University of Munich
Munich, Germany
michael.kramer@tum.de

ABSTRACT

The growing share of intermittent renewable energy sources together with the upcoming electrification of heating and cooling in European countries results in an increasing demand for operational flexibility in the energy system. Demand side management (DSM) of electric loads offers operational strategies to enable the provision of flexibility in demand of previously fixed loads. Residential electro-thermal heating systems are promising candidates to better utilize excess electricity generation from renewable energy sources, but may also add additional stress to existing grid infrastructure during peak load times. This paper introduces a bottom-up model to represent residential buildings in a district energy system. The operational behaviour of a model predictive control strategy is demonstrated, and its impact on the aggregate load curve is shown. The focus is on electro-thermal heating systems like heat pumps in Germany.

INTRODUCTION

Electro-thermal appliances such as heat pumps in combination with storages and the thermal mass of buildings can offer a certain load-shifting potential without seriously affecting the residents' comfort (Arteconi et al., 2013). Related previous work in the literature includes investigations on the potential of DSM on a single building level based on the physical characteristics of the thermal mass (Reynders et al., 2013) and evaluation of the economic operation of heat pumps in future power systems (Biegel et al., 2013).

In contrast to optimization models where electrical and thermal loads are treated as fixed input, studies to investigate the operational flexibility for DSM need a dynamic representation of the thermal behaviour of buildings. Lauster et al. (2014a) compare two dynamic building models by their accuracy and usability in city district simulations. Similar low-order models are developed by Reynders et al. (2014a) based on the Belgian residential building stock. Arteconi et al. (2016) use those models to investigate the impact of residential DSM of heat pumps on the Belgian energy market and demonstrate the applicability of low-order building models in a macro-level optimization problem.

There is a need for a better understanding of the local effects of electrified heating systems on distribution grids and how DSM mechanisms can be integrated into robust grid planning strategies. From a grid operator's perspective, individual building information is often limited to basic geographical information system (GIS) data and thus parameterization of detailed dynamic simulation models is challenging. Moreover, building properties within a building stock of an area might change over time. Consequently, parameterization by data provided by regional or national building typologies seems to be a promising approach for local bottom-up modeling.

In the optimal case, DSM as an operational measure is already taken into account during simulation studies in the planning phase. Since distribution grid operators are responsible for load forecasting in the corresponding energy supply area, a realistic representation of the operation must consider the receding horizon principle of the quarter-hourly balancing mechanism. Thus, a model predictive control (MPC) approach is suitable for simulating the behaviour of multiple buildings.

METHODOLOGY

The bottom-up approach presented in this paper creates single zone resistance and capacitance models to represent the dynamic behaviour of each building in Matlab. To account for diversity in the building stock, parameters like thermal transmittance values are based on a typology of the German residential building stock. Local scenarios for the penetration of electro-thermal heating systems can then be generated based on basic geometries and age class assumptions. The low-order models reduce the computational costs and still represent the most important dynamics.

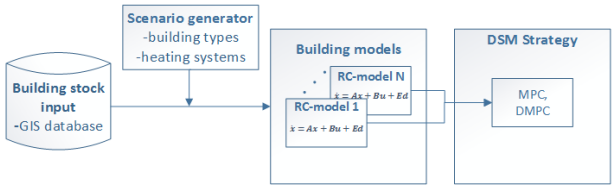

Figure 1:Workflow

For each building, a set of first order differential equations is stored and forwarded to the implementation of a control strategy, as depicted in Figure 1. A simple MPC strategy is derived to optimize the operation of each heating system. Finally, single building and aggregate simulation results for multiple buildings are presented for different price signals.

BUILDING TYPE SCENARIOS

Due to the lack of detailed information on parameters of individual buildings, a typology approach is used to generate representative datasets. The European research project *Typology Approach for Building Stock Energy Assessment* (TABULA) investigated the national residential building stocks with a harmonized approach to develop a comparable assessment for energy efficiency measures (Loga et al., 2015). The typology is organized by age classes and further distinguishes between single-family, multi-family, terraced houses and apartment buildings. A representative building description is given for each building type. For the purpose of this study, the most relevant TABULA cases are selected.

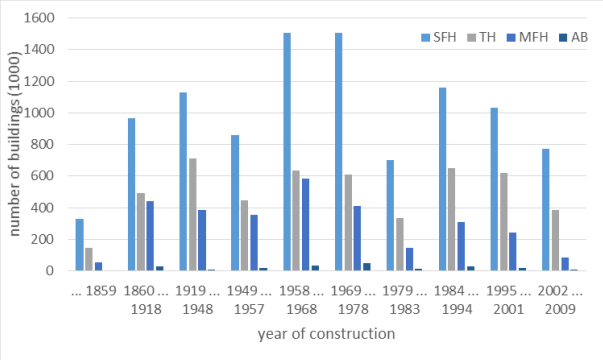

Figure 2: Distribution of the German national residential building stock based on Loga et al. (2015)

Figure 2 shows the distribution of building types of the German national building stock for constructions until the end of 2009. The periods were chosen with respect to the availability of statistical surveys, historical events and building regulations of relevance for thermal characteristics. With almost 10M buildings, single-family houses (SFH) represent 55% of all building types and approximately a third of all SFHs were constructed during the period from 1958 to 1978.

Every identified building type of the typology is described in three variants to account for different levels of refurbishment. All variants specify exemplary compositions of components of the building envelope (outer walls, floor, roof, window, door) and their overall value of thermal transmittance per square meter (U-value). The first variant describes the *existing state* with respect to the building regulation when the building was constructed. The variants *usual* and *advanced* refurbishment reflect the minimum requirements for refurbishments according to the regulation of the German Energy Saving Ordinance (EnEV) and low energy passive houses, respectively.

This paper only considers SFHs for two reasons. First, the development of low-order models based on building typologies has been limited to SFHs so far and the transferability of the modelling approach is not guaranteed for building types such as multi-family houses and apartment buildings, since they may have a very different thermal behaviour (Reynders et al., 2014a). Secondly, among residential space heating systems, electro-thermal heating systems have their highest share in SFHs in the existing stock and a third of all new build SFHs in Germany are equipped with heat pumps (Federal Statistical Office, 2016). SFHs are predominant in rural and suburban areas, where the low voltage grids are historically equipped with weaker infrastructure and face extensive connections of renewable resources and related grid disturbances (Büchner et al., 2014).

Local scenarios for the penetration of electro-thermal heating systems must account for both potential new buildings and refurbishments in the existing building stock that enable the installation of such heating systems. Besides remaining electrical night storage heaters from the 1950s and 1960s, heat pumps are the most frequently appearing electro-thermal technology. In a study on heat pump implementation scenarios in Europe, Bettgenhäuser et al. (2013) expect a growing market for heat pumps in Germany and assume an increasing share of air-to-water heat pumps to up to 59% of total annual heat pump sales, due to relatively low investment costs and limited space for ground-source heat pumps. In contrast to the TABULA study, which assumes air-source heat pumps as a possible alternative heating system in the usual refurbishment variant for every SFH type, Tenbohlen et al. (2015) argue, that only buildings constructed after 1995 are candidates for heat pumps. Since older buildings usually have higher design heat loads and in turn high supply temperatures, as a consequence fail to meet the requirements of low-temperature systems. An exception are buildings from 1958-1968 after refurbishment. A selection of TABULA cases most relevant to heat pump use in SFHs is summarized in Table 1.

Table 1: Selected building types from TABULA

Building type	**E SFH.05**	**J SFH.10**	**K SFH.11**	**L SFH.12**
Period	1958-1968	2002-2009	2010-2015	2016-
Refurbish-ment	(2) usual	(1) existing state	(1) existing state	(3) advanced
	U-value [W/m²K]			
Outer wall	0.23	0.30	0.24	0.11
Inner wall	2.33	0.36	0.36	0.36
Floor	0.31	0.28	0.35	0.13
Roof	0.42	0.25	0.22	0.11
Window	1.3	1.40	1.10	0.70
Door	1.31	1.99	1.75	0.80

Building type E in the variant of usual refurbishment represents existing buildings with improved thermal properties due to additional insulation and replaced windows as required by the EnEV 2009 for modernization. Types J and K represent newer SFHs constructed before and after the EnEV 2009/2014 in the basic setup. Building type L represents new constructions

in an advanced standard with an airtight envelope and a heat recovery system. This building type is comparable to nearly zero-energy buildings.
The modeling approach for single buildings is not restricted to the building types presented above and can be extended to any typologies as long as the necessary set of parameters is available.

BUILDING MODEL

Different methods exist to calculate the thermal behaviour of buildings. The main differences relate to the resulting accuracy and temporal resolution, necessary input data and computational requirements. Kämpf and Robinson (2007) classify explicit solutions, model reduction techniques and simplification methods as the three main categories of modelling approaches. Within simplification methods, thermal network models, which are based on an electrical circuit analogy are considered a good compromise between the above criteria and are thus often applied in the context of district energy analysis (Kämpf and Robinson, 2007; Lauster et al., 2014a). Well established low-order thermal network representations of whole buildings are described in the international standard ISO 13790 and German guideline VDI 6007. Since the latter offers a validated approach for transient simulations and has been successfully applied to works in the field of district energy analysis (see e.g. Lauster et al., 2014a), the building model presented in this paper is mainly based on the guideline VDI 6007.

Component modeling

The final building model lumps the main building components such as walls, floor, roof and windows together to a composition, which results in a model with few differential equations but acceptable accuracy. Therefore, the individual components have to be modeled first. For the periodic excitation case, the one-dimensional distribution of the heat flow $\underline{q}$ and the temperature $\underline{\vartheta}$ in a homogeneous wall layer for a coordinate x perpendicular to the wall can be expressed as

$$\begin{pmatrix} \underline{\vartheta}(x=0) \\ \underline{q}(x=0) \end{pmatrix} = A \begin{pmatrix} \underline{\vartheta}(x) \\ \underline{q}(x) \end{pmatrix}. \quad (1)$$

Thermal resistance per unit area, heat capacity per unit area and the period of the layer are input for the equations of chain matrix A. In the case of multiple wall or component layers ($v = 1, \dots, n$), matrix A_c for the entire wall or component can be calculated by matrix multiplication

$$A_c = A_1 \cdot A_2 \cdot \dots \cdot A_{n-1} \cdot A_n. \quad (2)$$

Furthermore, every component of a building can be represented by the 3R2C model depicted in Figure 3. The parameters R_1, R_2, R_3, C_1, C_2 can be directly calculated from matrix A_c and the area of the component. Further reductions are possible in cases where there are:

- Asymmetrically loaded components (outer walls, walls to zones of different temperatures): 2R1C
- Symmetrically loaded walls (inner walls): 1R1C

The workflow implemented in Matlab calls a function *component(materials, area)* for every building component presented in the final model. The function itself calls a function *layer(material)* for every wall layer in the component to create the corresponding chain matrix depending on the density ρ, heat capacity c, thermal conductivity λ and thickness s of the material of layer v. The above parameters and wall composition are stored for every building type and component shown in Table 1 in a database. Because the TABULA typology does not specify the exact building construction, common wall and material compositions are based on Arold (2014), Tenbohlen et al. (2015) and the ISO 10456.

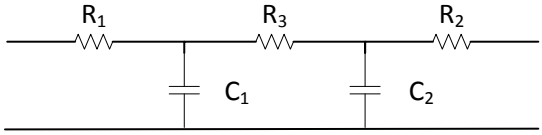

Figure 3: 3R2C model for a wall from VDI 6007

In the case of asymmetrically loaded components, the effective thermal mass must be carefully chosen to not overestimate the capacitance of the component model. Reynders et al. (2014b) suggest to only take into account the material layers within the insulation barrier, since only the first centimeters of an envelope wall are excited by a heating system. A more fundamental approach applied in this paper is presented in the VDI 6007, where the periodic depth of penetration is described by the period of a heat source, which in return affects the position and size of the resistances and capacity. The guideline recommends a period of seven days for building components and five days for the parallel connection of individual components.

Zone model of a building

The building is represented by a single zone model with a uniform air temperature in the whole zone. A function *building(typology, geometry)* generates a parameter set for the final low-order representation of the building. For a given geometry of a building, the function accesses the typology database and generates components for inner and outer walls, floors, door, roof and windows as described above. The editable geometry file includes among others the ground floor, outer wall and window areas, number of floors and floor height. The final model is shown in Figure 4. In contrast to the VDI 6007, which further reduces the model order to two capacitances for outer and inner walls, we keep the additional capacitances for simulation purposes.

$$\dot{T}_z = \frac{1}{R_{vent}C_z}(T_a - T_z) + \frac{1}{R_{wi}C_z}(T_{wi} - T_z) + \frac{1}{R_{wo,1}C_z}(T_{wo} - T_z) + \frac{1}{R_{fl,1}C_z}(T_{fl} - T_z) + \frac{s_z}{C_z}\varphi_{sg} + \frac{g_z}{C_z}\varphi_{ig} + \frac{f_z}{C_z}\varphi_{HP} \quad (3)$$

$$\dot{T}_{wi} = \frac{1}{R_{wi}C_{wi}}(T_z - T_{wi}) + \frac{s_{wi}}{C_{wi}}\varphi_{sg} + \frac{g_{wi}}{C_{wi}}\varphi_{ig} + \frac{f_{wi}}{C_{wi}}\varphi_{HP} \quad (4)$$

$$\dot{T}_{wo} = \frac{1}{R_{wo,2}C_{wo}}(T_{a,eq} - T_{wo}) + \frac{1}{R_{wo,1}C_{wo}}(T_z - T_{wo}) + \frac{s_{wo}}{C_{wo}}\varphi_{sg} + \frac{g_{wo}}{C_{wo}}\varphi_{ig} + \frac{f_{wo}}{C_{wo}}\varphi_{HP} \quad (5)$$

$$\dot{T}_{fl} = \frac{1}{R_{fl,2}C_{fl}}(T_g - T_{fl}) + \frac{1}{R_{fl,1}C_{fl}}(T_z - T_{fl}) + \frac{s_{fl}}{C_{fl}}\varphi_{sg} + \frac{g_{fl}}{C_{fl}}\varphi_{ig} + \frac{f_{fl}}{C_{fl}}\varphi_{HP} \quad (6)$$

Bacher and Madsen (2011) found that theoretically a minimum of two capacitances are necessary to cover short-term and long-term dynamics from parameter fitting of grey-box models. Reynders et al. (2015) found that due to the low-pass filtering effect of the high thermal mass, even a single capacitance model can provide a good approximation in the case of floor heating systems. In the case of modeling from building typologies and the absence of dynamic measurements, the presented structure is a reasonable starting point. A similar approach to create low-order building models from typology data was employed by Reynders et al. (2014a).

The parameters $R_{wo,1}$, $R_{wo,2}$ and C_{wo} are the thermal resistances and capacitance for all outer walls, which means a parallel connection of the envelope walls, roof, windows and door. R_{wi} and C_{wi} represent the inner walls with an area facing the zone equal to the outer walls. $R_{fl,1}$, $R_{fl,2}$ and C_{fl} represent the floor connected to the ground temperature T_g.

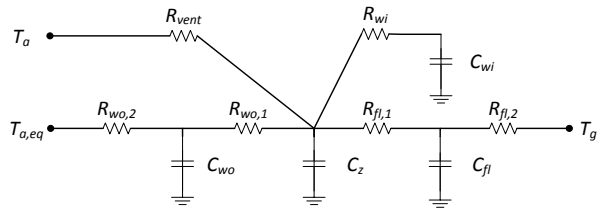

Figure 4: Single zone building model

In contrast to the VDI 6007, a capacitance of the zone C_z to summarize the heat capacity of the air volume and furniture at the zone temperature T_z is considered. Thermal bridges are considered with 0.1 W/m²K for the envelope area and lumped together with ventilation and infiltration losses in parameter R_{vent}. The losses are calculated according to Nielsen (2005) as $c_{air}V_{zone}(\eta_{vent} + \eta_{inf} + \eta_{mec}(1-\varepsilon))$, based on the heat capacity of air in the zone and the change rates η for natural ventilation, infiltration and, if present, mechanical ventilation with the efficiency of heat recovery ε. All final resistances include standard convective heat transfer coefficients at the surfaces. The short wave radiation on the building envelope is taken into account by the introduction of a modified equivalent ambient temperature

$$T_{a,eq} = T_a + (I_{dir} + I_{diff})\frac{\alpha_F}{\alpha_A} \quad (7)$$

with ambient temperature T_a, direct and diffuse radiation $I_{dir} + I_{diff}$ on the opaque outer wall areas and short-wave absorption and heat transfer coefficients α_F and α_A at the exterior surfaces. Solar gains φ_{sg} through windows are assumed to have a convective share of 9% (ISO 13790) added to the zone temperature T_z, the remaining fraction is split up according to an area-weighted distribution to the inner walls, outer walls and floor by the factors s. Likewise, the distribution of internal gains φ_{ig} from occupants and devices is carried out via factor f with a convective share of 50%.

Heating system

Further improvements regarding a linear consideration of the radiation heat transfer between interior and outer walls are discussed in Lauster et al. (2014b) and Harb et al. (2016). Especially for mainly radiative heating systems such as underfloor heating, an explicit consideration of the radiation processes could be useful but needs further investigation. Since the goal of this paper is an approximation of the thermal demand of a building, the interaction of the heating system with the building is simplified. The total power emitted from the heating systems φ_{HP} in case of a heat pump can be calculated as

$$\varphi_{HP} = COP_{HP}W_c \quad (8)$$

with the coefficient of performance COP_{HP} and the compressor power W_c. The coefficient of performance usually varies during the operation depending on the temperature conditions, but is treated as a constant input for the optimization in this study. Again, the radiative fraction of the heat input (95% in the case of underfloor heating) is distributed among the areas with the factors f_{wi}, f_{wo} and f_{fl}.

For every building, a design heat load calculation is carried out based on the simplified procedure of the DIN EN 12831. Transmission and ventilation heat losses are calculated for an ambient reference temperature, which represents an extreme local weather condition. Solar and internal gains are not considered in this procedure. The final heat load gives a limit for the maximum installed power $W_{c,max}$ of the heating system.

Building parameter set and state space model

Finally, the *building* function returns an individual set of parameters for the building components and heating system parameters. Temperatures T_{wi}, T_{wo} and T_{fl} are

defined at the capacitances. The differential equations of the low-order model lead to the equations (3)-(6). A state space representation of the model is used for the further design of the model predictive controller. In continuous-time, the differential equations can be rearranged to

$$\dot{x}(t) = A_c x(t) + B_c u(t) + E_c d(t) \quad (9)$$
$$\dot{y}(t) = C_c x(t). \quad (10)$$

with state vector $x = \left[T_z\ T_{wi}\ T_{wo}\ T_{fl}\right]^T$, control variable $u = W_c$, disturbance vector $d = \left[T_{a,eq}\ T_a\ T_g\ \varphi_{sg}\ \varphi_{ig}\right]^T$ and measured output $y = T_z$. Finally, the state space model of N_x states, N_u controllable inputs, N_d disturbances and N_y outputs has to be discretized to handle sampled data. Resulting matrices are indicated by the subscript "d", with $C_d = C_c$.

$$x_{k+1} = A_d x_k + B_d u_k + E_d d_k \quad (11)$$
$$y_k = C_d x_k \quad (12)$$

MODEL PREDICTIVE CONTROLLER DESIGN

The implemented MPC controller is based on the single building approach in Kramer et al. 2016 developed by the same authors. By reading in a building's state space model the extension enables the controller to handle any instance of model representing the discussed building types in Matlab. Model predictive control is an optimal control strategy to minimise a performance criterion such as costs or deviation from a trajectory, for a future time horizon. It is considered a good candidate for optimal temperature control in buildings, since it has the ability to treat multiple constrained input and output signals like weather conditions, occupancy, energy prices and building temperature states (Hazyuk et al. 2012). Its receding horizon fashion helps to handle deviations from forecasts.

In time step k, a prediction of the future model states $\hat{\boldsymbol{x}}_k = \left[\hat{x}_{k|k+1}, \hat{x}_{k|k+2}, \dots, \hat{x}_{k|k+N_P}\right]^T$ for all time steps of the prediction horizon N_P must be performed. From (11), future states can be derived as

$$\begin{aligned}\hat{x}_{k|k+1} &= A_d x_k + B_d u_k + E_d d_k \\ \hat{x}_{k|k+2} &= A_d \hat{x}_{k|k+1} + B_d u_{k|k+1} + E_d \hat{d}_{k|k+1} \\ &= A_d^2 x_k + A_d B_d u_k + B_d u_{k|k+1} \\ &\quad + A_d E_d d_k + E_d \hat{d}_{k|k+1}. \end{aligned} \quad (13)$$

(13) shows that the future states can be estimated based on the current state in k, current and future controllable input and the forecast of the disturbances. All future $N_x N_P$ states can be estimated by

$$\hat{\boldsymbol{x}}_k = \phi x_k + \Gamma \boldsymbol{u}_k + K \hat{\boldsymbol{d}}_k \quad (14)$$

with

$$\phi = \begin{bmatrix} A_d \\ A_d^2 \\ \vdots \\ A_d^{N_P} \end{bmatrix}$$

$$\Gamma = \begin{bmatrix} B_d & 0 & 0 & \cdots & 0 \\ A_d B_d & B_d & 0 & \cdots & 0 \\ A_d^2 B_d & A_d B_d & B_d & \cdots & 0 \\ \vdots & \vdots & \vdots & \ddots & 0 \\ A_d^{N_P-1} B_d & A_d^{N_P-2} B_d & A_d^{N_P-3} B_d & \cdots & B_d \end{bmatrix}$$

$$K = \begin{bmatrix} E_d & 0 & 0 & \cdots & 0 \\ A_d E_d & E_d & 0 & \cdots & 0 \\ A_d^2 E_d & A_d E_d & E_d & \cdots & 0 \\ \vdots & \vdots & \vdots & \ddots & 0 \\ A_d^{N_P-1} E_d & A_d^{N_P-2} E_d & A_d^{N_P-3} E_d & \cdots & E_d \end{bmatrix}$$

of dimensions $\phi \in \mathbb{R}^{N_x N_P \times N_x}$, $\Gamma \in \mathbb{R}^{N_x N_P \times N_u N_P}$ and $K \in \mathbb{R}^{N_x N_P \times N_d N_P}$. The estimated zone temperature as the output signal can be computed as

$$\hat{\boldsymbol{y}}_k = C \hat{\boldsymbol{x}}_k \quad (15)$$

with

$$C = \begin{bmatrix} C_d & 0 & \cdots & 0 \\ 0 & C_d & \cdots & 0 \\ \vdots & \vdots & \ddots & 0 \\ 0 & 0 & 0 & C_d \end{bmatrix}$$

of dimension $C \in \mathbb{R}^{N_P \times N_x N_P}$.

The objective function chosen for the controller is total energy costs. In every time step, the controller minimises the sum of consumed compressor power multiplied by a price vector p over the given prediction horizon N_P.

$$J_{energy\ costs} = \sum_{k=1}^{Np} p_k W_{c,k}\, \Delta t \quad (16)$$

Formula (14) is incorporated as an equality constraint for the final optimization problem. The zone temperature T_z must stay within the range between 19 °C and 21 °C, which is represented by an inequality constraint. The complete mathematical formulation is detailed in Kramer et al. 2016.

SIMULATION RESULTS

A validation of the exact thermal behaviour for a single building model is beyond the scope of this paper. Validation results for low-order models parameterized by a typology can be found in Reynders et al. (2014a). The following simulation results demonstrate the implementation of the controller for the chosen building types.

The low-order models for all types are created with building geometries of type J for comparability. Parameters are summarized in Table 2. The design heat load calculation is performed for the city of Munich and

representative weather data is generated from Meteonorm. The ground temperature is assumed to be constant at 10 °C and the initial states are $x_0 = [20\ 20\ 20\ 20]^T$.
The MPC is simulated for six consecutive days in January with a temporal resolution of 15 minutes. This is also the discretization time-step for the system dynamics in equation (11). Perfect prediction of all disturbances within the next 24 hours is assumed for all simulations.

Table 2: Type specific parameters and geometry

Building type	**E SFH.05**	**J SFH.10**	**K SFH.11**	**L SFH.12**
Thermal bridges [W/m²K]	0.1	0.05	0.05	0.02
$\eta_{vent} + \eta_{inf}$ [1/h]	0.6	0.5	/	/
η_{mec} [1/h] ε [ ]	/	/	0.55 0.84	0.55 0.84
$\dot{Q}_{Heat\ load}$ [kW]	8.39	7.38	4.87	2.65
	Area [m²]			
Outer wall	188.9			
Inner wall	188.9			
Floor	79.8			
Roof	85.9			
Window N/S/E/W	3.1 / 17.3 / 3.9 /3.9			
Door	2			

In contrast to the ambient temperature and global radiation, which are disturbances that are assumed to be the same for all buildings within an area, the internal gains over the day may differ among individual buildings and lead to additional diversity in the heat demand. At this stage, the internal gains are modeled in a simplified way and only cover the radiative and convective components from occupants in a three-person household. A period of inactivity or sleep is defined between 11 p.m. and 6 a.m. with 80 W per person injected to the zone. During the rest of the day, occupancy is uniformly distributed and assumed to result in a random heat gain between 100 and 125 W per person, which corresponds to values of sedentary occupation (VDI 2078, 2015). Time dependency on occupancy and activities are not considered.

Single buildings - constant price

Figure 5 shows the simulation results for the selected SFH types for a constant electricity price. The constant price implies that the total energy costs can only be minimised by reducing the heat pump operation to the possible minimum without violating the comfort temperature band. By keeping the price constant, the operation is only optimized with respect to the disturbances. For all building types, T_z is always kept within its limits, most of the times being exact 19 °C to minimize the consumption of the heat pump and thus total energy cost. W_c is optimized to a minimum operation by forecasting the sequence of the disturbances. It is possible to switch off or at least reduce the compressor power when the daily solar radiation peak occurs. This effect is less pronounced for the building types E and J, of which inferior insulation results in a higher power injection and a longer operation time compared to building type L, which has the shortest on-time. The superior insulation of type L is also observed through the impact of the solar radiation peak on the zone temperature. Compared to the types E, J and K the solar gain (mainly transferred by the large south oriented window) results in a higher net heat transfer for type L, since simultaneous thermal losses are lower.
The heat pump operation is mainly driven by the ambient temperature and solar radiation, which are the same for all building types simulated. The internal gains have only a minor impact. This leads to a high coincidence of the resulting power demand for the four buildings. It is obvious that under the assumption of a constant price signal and the usage of similar controllers in multiple buildings will result in a high aggregate local demand.

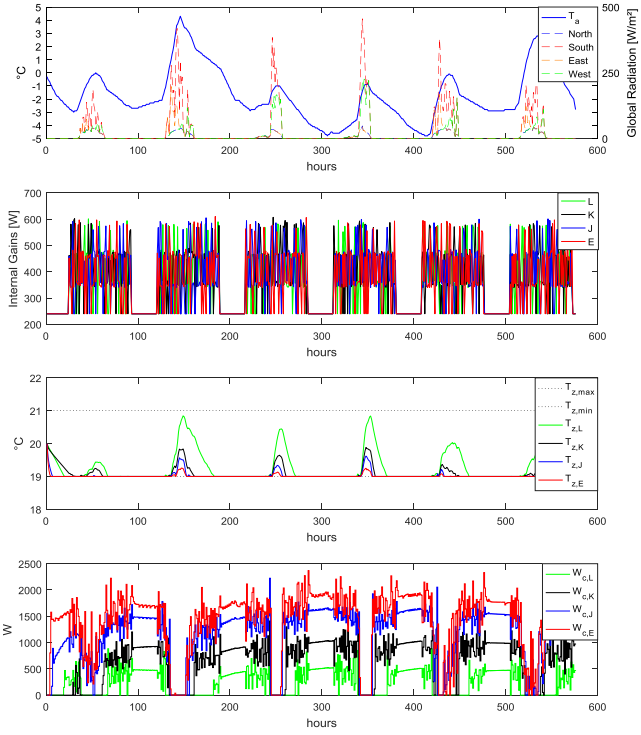

Figure 5: Simulation results for SFH types L, K, J and E for a constant price

Multiple buildings - time varying price signal

The previous discussion leads to a simulation case study for the aggregation of multiple buildings equipped with heat pumps. The aggregation is assumed to consist of 100 three-person households, each of them living in a single family house. For the comparison to a reference electrical load curve, 100 individual electricity profiles are generated from the residential electricity model of Jambagi et al. (2015) and aggregated. The profiles account for the fixed electricity demand of household appliances excluding demand for electric heating systems

like heat pumps. Standard household appliances such as fridges, dishwashers, washing machines and entertainment devices are assumed to be inflexible. Figure 6 shows the aggregate of the fixed electrical loads for the 100 households in a temporal resolution of 15 minutes. The fixed load curve (FLC) shows typical peaks of the residential demand during noon and evening hours. In a worst-case scenario, the additional electricity demand from heat pumps would add up to the peak demand of the fixed loads. Intuitively, to aim for a flat electricity demand profile, the shape of the fixed load curve can be used as a time-varying price signal as it indicates times of low and high prices according to the fixed demand. Thus, to prevent clustering of additional heat pump demand, the fixed load curve is used as a simple time-varying price vector in equation (16).

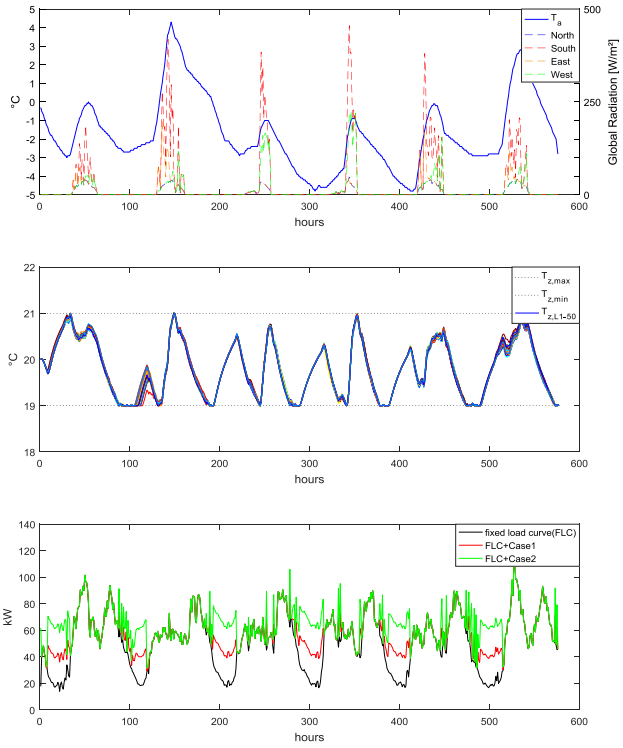

Figure 6: Simulation results for 100 households, a time-varying price and 25% (Case 1) / 50% (Case 2) penetration rates in SFHs, type L

The results in Figure 6 show the aggregated electricity demand before and after buildings are equipped with heat pumps. The penetration rates indicate the percentage of SFHs that have a heat pump:

- Case 1: 25% of all 100 SFHs type L
- Case 2: 50% of all 100 SFHs type L

The MPC optimizes the operation of each heat pump consecutively. The same reference aggregated load curve (FLC) is used as a price signal for each optimization. In both cases, the operation of the heat pumps is mainly shifted to low demand times of the FLC, since here the lowest prices are offered. The resulting peak demand of the sum of the FLC and the heat pumps never exceeds the all-time peak demand on day six without heat pumps. Operational flexibility is provided by the thermal inertia of the buildings and the use of the full temperature range for T_z. The latter is depicted in Figure 6 for all 50 buildings with heat pumps in case 2. It can be observed that the single temperature trajectories differ significantly in comparison to $T_{z,L}$ from Figure 5, due to the time-varying price and a new schedule for the heat pump operation. Since only the internal gains differ among buildings and all other disturbances and the price signal are the same for every building's optimization, there is little variation of temperatures and compressor power trajectories among the buildings. This leads to a high coincidence of the heat pumps aggregate demand. Especially for case 2, this causes steep load gradients before and after times of low price. The results indicate that such a simple price signal will not be sufficient for higher penetration rates of heat pumps or buildings with inferior insulation and higher demands. Simulation results for type E showed exceedance of the peak demand for penetration rates below 25%.

CONCLUSION

The developed bottom-up approach provides a simulation framework for distribution grid operators to investigate realistic scenarios for the future penetration of residential electro-thermal heating systems and to test DSM strategies to mitigate their impact. The results show that a typology approach is successful in parameterizing low-order building models and accounting for possible diversity in the local building stock. The proposed MPC controller demonstrates how the demand of additional heat pumps can have a massive impact on the aggregate load curve, but also shows how a suitable price signal can lead to a shift of demand to mitigate stress on distribution grids.

Further work will include a more detailed representation of the heat pump heating system, including a time varying COP. As domestic hot water provision from heat pumps was not included in this study, further work will extend the building model and the MPC algorithm to cover the full electricity demand. Finally, to quantify the optimal distribution of the load, further DSM strategies for the aggregate of multiple buildings will be investigated.

REFERENCES

Arold, J. (2014). Perspektiven von Strom zur Wärmeerzeugung in Niedrigstenergiegebäuden. Dissertation, University of Stuttgart 2014.

Arteconi, A., Hewitt, N.J. and Polonara, F. (2013). Domestic demand-side management (DSM): Role of heat pumps and thermal energy storage (TES) systems. In *Applied Thermal Engineering, 51*(12), 155–165.

Arteconi, A., Patteeuw, D., Bruninx, K., Delarue, E., D'Haeseleer, W., Helsen, L. (2016). Active demand response with electric heating systems: impact of market penetration. In *Applied Energy 177 (2016)*, 636-648.

Bacher, P., Madsen, H. (2011) Identifying suitable models for the heat dynamics of buildings. In *Energy and Buildings* 43 (2011), 1511-1522.

Bettgenhäuser, K. Offermann, M., Boermans, T., Bosquet, M., Grözinger, J., von Manteuffel, B., Surmeli, N. (2013). Heat Pump Implementation Scenarios until 2030. Project report. Ecofys Germany GmbH, Cologne.

Biegel, B., Andersen, P., Pedersen, T.S., Nielsen, K.M., Stoustrup, J., Hansen, L.H. (2013). Electricity Market Optimization of Heat Pump Portfolio. In Proc. *2013 IEEE International Conference on Control Applications*, Hyderabad, 294-301.

Büchner, J., Katzfey, J. Flörcken, O. Moser, A., Schuster, H., Dierkes, S., van Leeuwen, T., Verhegg, L., Uslar, M., Amelsvoort, M. (2014). Moderne Verteilernetze für Deutschland“ (Verteilernetzstudie). Study for the Federal Ministry for Economic Affairs and Energy.

Federal Statistical Office (2016). Bautätigkeit und Wohnungen 2015. Fachserie 5 Reihe 1. Wiesbaden.

Guideline VDI 2078 (June 2015), Düsseldorf: Beuth Verlag.

Guideline VDI 6007-1 (June 2015), Düsseldorf: Beuth Verlag.

Harb, H., Boyanov, N., Hernandez, L. Streblow, R., Müller, D. (2016). Development of grey-box models for forecasting the thermal response of occupied buildings. In *Energy and Buildings* 117 (2016), 199-207.

Hazyuk, I., Ghiaus, C., Penhouet, D. (2012). Optimal temperature control of intermittently heated buildings using Model Predictive Control: Part II – Control Algorithm. In *Building and Environment* 51 (2012), 388-394.

International Standard DIN EN ISO 10456:2007, Berlin: Beuth Verlag.

International Standard DIN EN ISO 12831:2012, Berlin: Beuth Verlag.

International Standard DIN EN ISO 13790:2008, Berlin: Beuth Verlag.

Jambagi, A., Kramer, M., Cheng, V. (2015). Residential Electricity Demand Modelling: Activity based modelling for a model with high time and spatial resolution, In Proc. *3rd International Renewable and Sustainable Energy Conference (IRSEC)*, 10-13 December 2015, Marrakech & Ouarzazate, Morocco.

Kämpf, J.H., Robinson, D. (2007). A simplified thermal model to support analysis of urban resource flows. In *Energy and Buildings* 39 (2007), 445-453.

Kramer, M., Jambagi, A., Cheng, V. (2016). A model predictive control approach for demand side management of residential power to heat technologies. In. Proc. *2016 IEEE International Energy Conference (ENERGYCON), Leuven.*

Lauster, M., Teichmann, J., Fuchs, M., Streblow, R. Mueller, D. (2014a). Low order thermal network models for dynamic simulations of buildings on city district scale. In *Building and Environment* 73 (2014), 223-231.

Lauster, M., Brüntjen, M.-A., Leppmann, H., Fuchs, M., Teichmann, J., Streblow, R., van Treeck, C., Mueller, D. (2014b). Improving a low order building model for urban scale applications. In Proc. *Fith German-Austrain IBPSA Consference BauSIM 2014*, Aachen, 511-518.

Loga, T., Stein, B., Diefenbach, N., Born, R. (2015). Deutsche Wohngebäudetypologie. Beispielhafte Maßnahmen zur Verbesserung der Energieeffizienz. von typischen Wohngebäuden. Institut Wohnen und Umwelt, Darmstadt.

Nielsen, T.R. (2005). Simple tool to evaluate energy demand and indoor environment in the early stages of building design. In *Solar Energy* 78 (2005), 73-83.

Reynders, G., Nuytten, T., Saelens, D. (2013). Potential of structural thermal mass for demand-side management in dwellings. In *Energy and Buildings* 64 (2013), 188-197.

Reynders, G., Diriken, J., Saelens, D. (2014a). Bottom-up modeling of the Belgian residential building stock: influence of model complexity. In Proc. *International conference on system simulation in buildings*, Edition 9, Liège, 574–92.

Reynders, G., Diriken, J., Saelens, D. (2014b). Quality of grey-box models and identified parameters as function of the accuracy of input and observation signals. In *Energy and Buildings* 82 (2014), 263–274.

Reynders, G., Diriken, J., Saelens, D. (2015). Impact of the heat emissions system on the identification of grey-box models for residential buildings. In *Energy Procedia* 78 (2015), 3300-3305.

Tenbohlen, S., Brunner, M., Schmidt, M., Henzler, T. (2015). Be- und Entlastung elektrischer Verteilnetze durch Wärmepumpen bei der Wärmeerzeugung in Wohngebäuden. University of Stuttgart.